

Search for narrow resonances below the Υ mesonsG. Apollinari,² M. Barone,¹ W. Carithers,⁴ M. Dell'Orso,⁵ T. Dorigo,⁶ I. Fiori,⁵ M. Franklin,³ P. Giannetti,⁵ P. Giromini,¹ F. Happacher,¹ S. Miscetti,¹ A. Parri,¹ F. Ptohos,^{1,*} and G. Velev²¹*Laboratori Nazionali di Frascati, Istituto Nazionale di Fisica Nucleare, Frascati, Italy*²*Fermi National Accelerator Laboratory, Batavia, Illinois 60510, USA*³*Harvard University, Cambridge, Massachusetts 02138, USA*⁴*Ernest Orlando Lawrence Berkeley National Laboratory, Berkeley, California 94720, USA*⁵*Istituto Nazionale di Fisica Nucleare, University and Scuola Normale Superiore of Pisa, I-56100 Pisa, Italy*⁶*Istituto Nazionale di Fisica Nucleare, Università di Padova, Sezione di Padova, I-35131, Padova, Italy*
(Received 10 August 2005; revised manuscript received 18 October 2005; published 16 November 2005)

We have investigated the invariant mass spectrum of dimuons collected by the CDF experiment during the 1992–1995 run of the Fermilab Tevatron collider to improve the limit on the existence of narrow resonances set by the experiments at the SPEAR e^+e^- collider. In the mass range $6.3 - 9.0 \text{ GeV}/c^2$, we derive 90% upper credible limits to the ratio of the production cross section times muonic branching fraction of possible narrow resonances to that of the $\Upsilon(1S)$ meson. In this mass range, the average limit varies from 1.7 to 0.5%. This limit is much worse at the mass of $7.2 \text{ GeV}/c^2$ due to an excess of 250 ± 61 events with a width consistent with the detector resolution.

DOI: [10.1103/PhysRevD.72.092003](https://doi.org/10.1103/PhysRevD.72.092003)

PACS numbers: 13.20.Gd, 13.60.Le

I. INTRODUCTION

Supersymmetric theories provide a mechanism to break the electroweak symmetry and to stabilize the large hierarchy between the Planck and the Fermi scales. Supersymmetry requires the existence of scalar partners to each standard model (SM) fermion, and spin $-1/2$ partners to the gauge and Higgs bosons. In particular, supersymmetry predicts the existence of scalar quarks, i.e. particles that carry color, but no spin. Scalar quarks (squarks) have been searched for at current and past colliders, but charge $-1/3$ squarks might have been overlooked for several reasons. Within the minimal supersymmetric standard model (MSSM), Ref. [1] shows that the existence of a yet undetected charge $-1/3$ scalar quark, lighter than the b quark, would require a lot of fine-tuning of the MSSM parameters, but at present cannot be ruled out by the electroweak precision data and the Higgs mass constraints from LEP2. Charge $-1/3$ squarks would give a 2% contribution to the inclusive cross section for $e^+e^- \rightarrow$ hadrons; this contribution is comparable to the experimental error of the present measurements [2,3]. Searches for narrow resonances at SPEAR have set upper bounds on Γ_l , the leptonic width of possible resonances, of 100 eV in the mass region $5.7 \leq E_{\text{cm}} \leq 6.4 \text{ GeV}$ and of approximately 60 eV in the region $7.0 \leq E_{\text{cm}} \leq 7.4 \text{ GeV}$ [4]. In Ref. [5], the leptonic width of 1^{--} bound states of such squarks has been evaluated using potential models of ordinary heavy quarks [6]. Because of the p -wave suppression of the fermion contribution to their decay width, the leptonic width is estimated to be approximately 18 (6) eV for a resonance with a 6 (10) GeV/c^2 mass. As noted in Ref. [5], for quarkonium masses above $6 \text{ GeV}/c^2$ the width

Γ_l is well below the experimental bounds, and scalar-quark resonances might have been missed. With this study, we investigate the region above $6.3 \text{ GeV}/c^2$ by using muon pairs with invariant mass between the ψ and Υ mesons. The large statistics data set has been collected with the Collider Detector at Fermilab (CDF) during the 1992–1995 Fermilab collider run. Section II describes the detector systems relevant to this analysis. Section III reviews the expectation for bound states of charge $-1/3$ squarks. The data sample is described in Sec. IV, and Sec. V presents additional selection criteria, tuned with $\Upsilon(1S)$ decays, which reduce the nonresonant background by a factor of three without losing more than 10% of the signal. In Sec. VI, we fit the dimuon invariant mass distribution and derive a 90% Bayesian upper limit on Γ_l as a function of the resonance mass. The shape of the invariant mass distribution is generally quite smooth and we improve the SPEAR limit by an order of magnitude. An exception is the mass of $7.2 \text{ GeV}/c^2$, at which the data can accommodate a Gaussian bump of 250 ± 61 events. In Sec. VII we explore the possibility of observing a real signal, we estimate its statistical significance, and we study its robustness by using a number of different kinematical selections. Our conclusions are summarized in Sec. VIII.

II. CDF DETECTOR

CDF is a multipurpose detector, equipped with a charged particle spectrometer and a finely segmented calorimeter. In this section, we recall the detector components that are relevant to this analysis. The description of these subsystems can be found in Ref. [7]. Two devices inside the 1.4 T solenoid are used for measuring the momentum of charged particles: the silicon vertex detector (SVX) and the central tracking chambers (CTC). The SVX consists of four con-

*Present address: University of Cyprus, 1678 Nicosia, Cyprus.

centric layers of silicon microstrip detectors surrounding the beam pipe. The CTC is a cylindrical drift chamber containing 84 sense wire layers grouped into nine alternating superlayers of axial and stereo wires. Electromagnetic (CEM) and hadronic (CHA) calorimeters surround the tracking volume and measure energy deposits over the pseudorapidity region $|\eta| \leq 1$. Muons are reconstructed by matching track segments in the drift chamber systems located outside the CHA (CMU, CMP, and CMX muon detectors, which cover the region $|\eta| \leq 1$) to the tracks of charged particles reconstructed in the CTC. The dimuon events used in this analysis were collected with a three-level trigger system. The first level required two charged tracks in the muon chambers. The second level trigger required that both muon tracks match a charged particle with transverse momentum $p_T \geq 2.2$ GeV/c as measured by a fast track processor (CFT). The third level software trigger requires that two charged CTC tracks, fully reconstructed in three dimensions, match track segments in the muon chambers and that the dimuon invariant mass is larger than 2.8 GeV/c².

III. SEARCH FOR NARROW RESONANCES

In this study, we search for narrow resonances ε , bound states of scalar quarks, in the dimuon invariant mass distribution between 6.3 and 9.0 GeV/c². For a charge $-1/3$ squark, the muonic width, $\Gamma_\mu(\varepsilon \rightarrow \mu^+ \mu^-)$, of $2P$ resonances in this mass range has been evaluated in Ref. [5] to be approximately 15 eV. In contrast, the $Y(1S)$ meson has a larger leptonic width Γ_μ of 1.32 keV. In analogy with the $Y(1S)$ meson, the annihilation of an ε state into hadrons is believed to proceed through gluons [5], the dominant contribution coming from the minimum number of intermediate gluons (one-gluon is excluded by color conservation and two-gluons by C-conservation). In $p\bar{p}$ collisions quarkonia states are directly produced through subprocesses such as $g\bar{g} \rightarrow gY(1S)$ or $g\bar{g} \rightarrow g\varepsilon$. As the production subprocesses are directly related by crossing to the corresponding decay processes, the production cross section σ is determined by the decay widths [8], and approximately reads:

$$\begin{aligned} \sigma_\varepsilon B(\varepsilon \rightarrow \mu\mu) &\simeq \left(\frac{m_{Y(1S)}}{m_\varepsilon}\right)^3 \frac{\Gamma_\mu^\varepsilon}{\Gamma_\mu^{Y(1S)}} \sigma_{Y(1S)} B(Y(1S) \rightarrow \mu\mu) \\ &= R \sigma_{Y(1S)} B(Y(1S) \rightarrow \mu\mu), \end{aligned} \quad (1)$$

where B is the branching ratio of the muonic decay and $R = \left(\frac{m_{Y(1S)}}{m_\varepsilon}\right)^3 \frac{\Gamma_\mu^\varepsilon}{\Gamma_\mu^{Y(1S)}}$. For an ε particle in the mass region investigated by this study, R is approximately 2% when the width Γ_μ^ε is evaluated using the standard potential of heavy-quark spectroscopy [5]. Using a different potential model and one-loop corrections to the static potential of the scalar quark-anti-quark system, Ref. [9] predicts leptonic widths that are a factor of three larger. In conclusion, R is expected to be between 2 and 6% . Since CDF has

collected approximately 10^4 $Y(1S)$ mesons, the data could contain at least 200 events contributed by a hypothetical ε meson on top of the smooth background due to Drell-Yan production, double semileptonic decays of $c\bar{c}$ and $b\bar{b}$ pairs, and fake muons produced by hadrons that mimic their signal.

IV. DIMUON DATA SAMPLE

The dimuon sample used in this analysis corresponds to approximately 110 pb⁻¹ of data collected with the CDF detector during the 1992–1995 collider run. This data set has been used in several CDF analyses and is described in more detail in Ref. [10]. The muon identification is based on the three-dimensional matching of the track segment in the muon chambers with the track reconstructed in the CTC and on the energy deposited in the calorimeter tower in the muon path [10,11]. In this study, we search for muons with $p_T \geq 3$ GeV/c using the same selection criteria of Ref. [11]; we select muons with $2 \leq p_T \leq 3$ GeV/c using the stricter cuts of the SLT algorithm [12,13] in order to reduce the misidentification background. We require that at least one of the muons is identified by both the CMP and CMU systems ($p_T \geq 3$ GeV/c and pseudorapidity $|\eta| \leq 0.6$). Additional muons are identified by either the CMU or CMX system ($p_T \geq 2$ GeV/c and $|\eta| \leq 1.0$). These selection criteria yield reconstructed muon pairs with rapidity $|y| \leq 1.0$. We retain events which contain two and only two muons. The muon momentum is evaluated with a fit which constrains the track to originate from the beam line. The dimuon invariant mass is calculated using these momenta. This study uses opposite charge dimuon pairs; however, distributions for same charge dimuon pairs are also shown as a cross-check.

The dimuon invariant mass distribution is shown in Fig. 1. The yield of ψ mesons is much suppressed with respect to that of Y mesons. Because of the muon selection criteria, at the J/ψ mass the kinematic acceptance decreases rapidly with J/ψ decreasing transverse momentum and vanishes at $p_T \simeq 5$ GeV/c. In contrast, for muon pairs with invariant masses larger than 6.3 GeV/c², the kinematic acceptance does not depend on the dimuon transverse momentum. Therefore, we avoid the uncertainty of modeling an acceptance that depends on the production kinematics by limiting our study to the mass region above 6.3 GeV/c². The dimuon invariant mass distribution at the $Y(1S)$ and in the region of interest for this study are shown in Fig. 2. The number of $Y(1S)$ mesons in the data is derived by fitting a first order polynomial and a Gaussian function to the invariant mass distribution in Fig. 2 with a binned maximum likelihood method. The best fit returns $9838 \pm 141 Y(1S)$ mesons over a background of 5769 events in the region $9.3 \leq M_{\mu^+ \mu^-} \leq 9.55$ GeV/c². The fit also returns $M_{Y(1S)} = 9439 \pm 1$ MeV/c² and a mass resolution $\sigma_M = 57 \pm 1$ MeV/c². This mass resolution

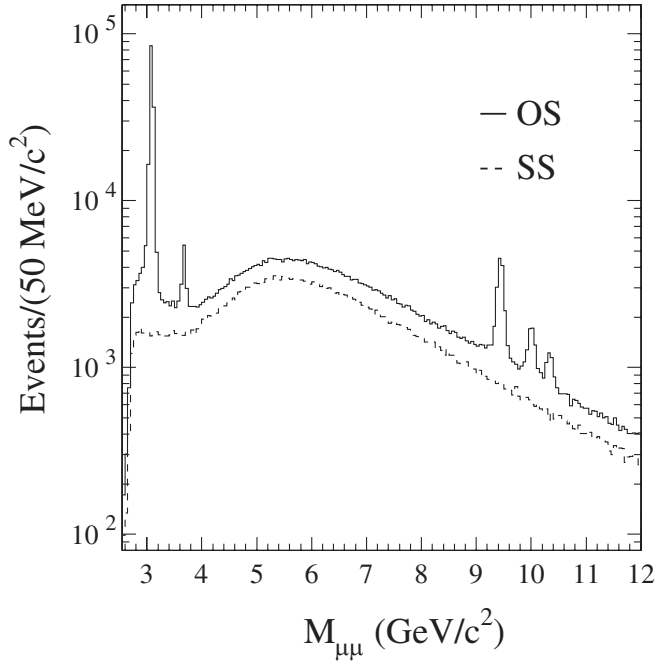


FIG. 1. Invariant mass distribution of all muon pairs. OS indicate dimuons with opposite sign charge used in this analysis. Dimuons with same sign charge (SS) are also shown.

is well modeled by a simulation of the process $p\bar{p} \rightarrow Y(1S)X$. The simulation event generator produces $Y(1S)$ mesons with the transverse momentum distribution of the data [14] and a flat rapidity distribution for $|y| \leq 1$. The generated events are processed with the CDF detector simulation¹ (QFL) described in detail in Ref. [15]. Events are then required to pass the same selection and reconstruction criteria imposed on the data. This simulation predicts a mass resolution of 40 MeV/c^2 for ϵ states with a mass around 7.5 GeV/c^2 .

V. BACKGROUND REDUCTION

As outlined in Sec. III, the hypothetical signal of an ϵ resonance of mass $\approx 7.5 \text{ GeV}/c^2$ is expected to be at least 2% of the $Y(1S)$ yield, i.e. about 200 events. Given the detector invariant mass resolution, the 200 events have to be integrated in a region of 150 MeV/c^2 ($\pm 2\sigma_M$). As shown in Fig. 2, three 50 MeV/c^2 bins centered around this mass contain approximately 8000 events. This background can be largely suppressed because it is mostly contributed by $b\bar{b}$ and $c\bar{c}$ production. The measurement of the time-integrated $B^0 - \bar{B}^0$ mixing probability, reported in Ref. [16], also makes use of this data sample.

¹The simulation includes correction factors for the efficiency of the three-level trigger system, the efficiency for reconstructing tracks in the CTC and the different muon systems, effects due to instantaneous luminosity and to internal radiation from muons. These correction factors are parametrizations based on the data [14,15].

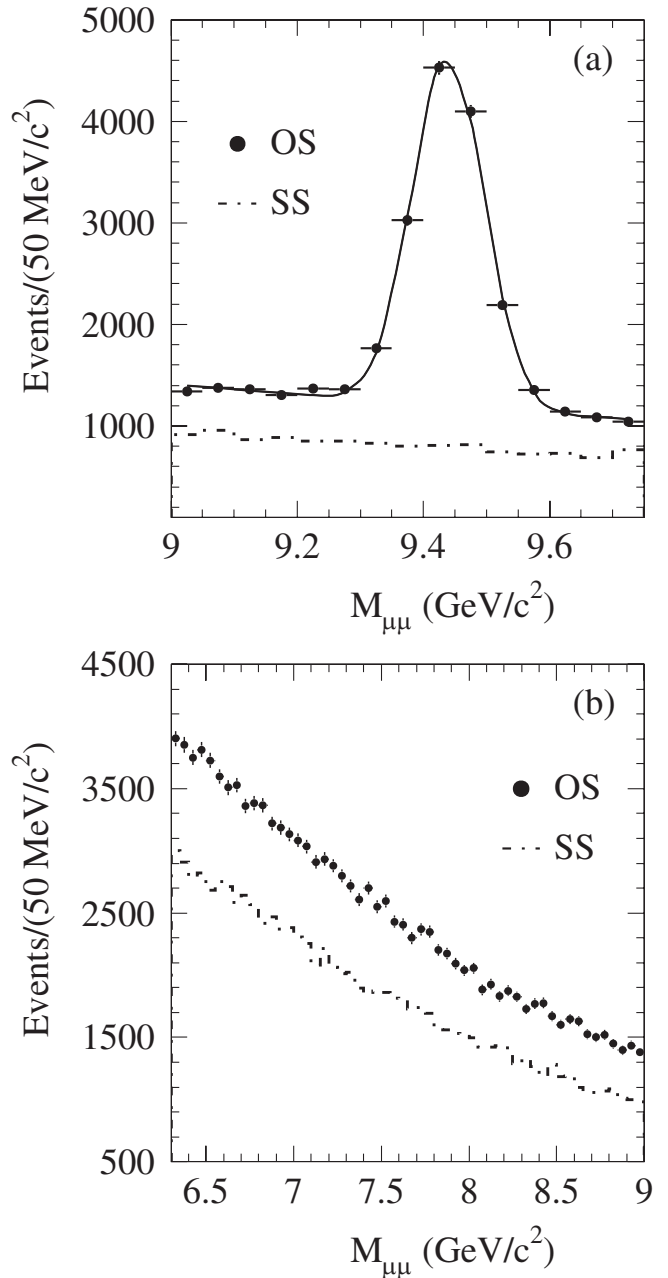


FIG. 2. Invariant mass distributions of muon pairs at the $Y(1S)$ (a) and in the region of interest for this study (b). The solid line represents the fit used to estimate the number of $Y(1S)$ mesons.

From that study we estimate that approximately 75% of the muon pairs arise from heavy flavor production. We use two intuitive criteria to reject dimuons arising from the decay of hadrons with heavy flavor:

- (1) An isolation requirement. The isolation, I , is defined as the scalar sum of the transverse momenta of all the tracks in a cone of radius $R = \sqrt{\delta\phi^2 + \delta\eta^2} = 0.4$ around the muon direction. We require that both muons have isolation $I \leq 4 \text{ GeV}/c$.
- (2) A promptness requirement. In contrast to b and c -hadrons, the $Y(1S)$ and ϵ mesons have negligible

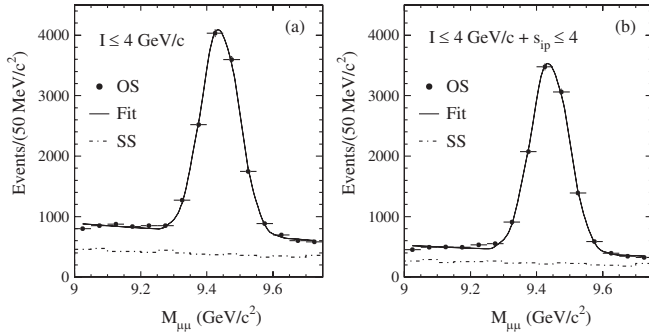


FIG. 3. Invariant mass distributions of opposite (\bullet) and same sign charge (dot-dashed) muon pairs in the $Y(1S)$ mass range after the isolation (a) and impact parameter cuts (b). The solid line is a fit using a Gaussian plus a first order polynomial functions.

TABLE I. Numbers of $Y(1S)$ mesons and underlying-background events for different analysis cuts. Rates are evaluated by fitting the data with a Gaussian plus a first order polynomial function. The background is integrated over the mass region between 9.3 and 9.55 GeV/c^2 . The last cut, QC , is used in the ε search. Efficiencies are calculated with respect to the number of $Y(1S)$ candidates in the first row.

| Cut | $Y(1S)$ candidates | Background | Efficiency (%) |
|-------------------|--------------------|------------|----------------|
| None | 9838 ± 141 | 5769 | |
| I | 9821 ± 129 | 3345 | 99.8 |
| $QC = I + s_{ip}$ | 9064 ± 118 | 1842 | 92.1 |

lifetime. We select prompt muons by requiring the sum of the impact parameter significance of both muons, s_{ip} , to be less than 4^2 . The impact parameter significance is estimated for muons with tracks reconstructed in the microvertex silicon detector (SVX), otherwise is set to zero in order not to lose events.

The values of these cuts have been determined at the $Y(1S)$ mass (see Fig. 3). As shown in Table I, these cuts reduce the background by more than a factor of three while retaining more than 90% of the $Y(1S)$ signal.

VI. ESTIMATE OF THE UPPER LIMIT ON Γ_I^ε

Figure 4 shows the invariant mass distribution of muon pairs in the region between 6.3 and 9.0 GeV/c^2 after the isolation and impact parameter significance cuts.

We use a binned maximum likelihood method to fit the mass spectrum in Fig. 4 with a fourth order polynomial, which serves the purpose of modeling a smooth back-

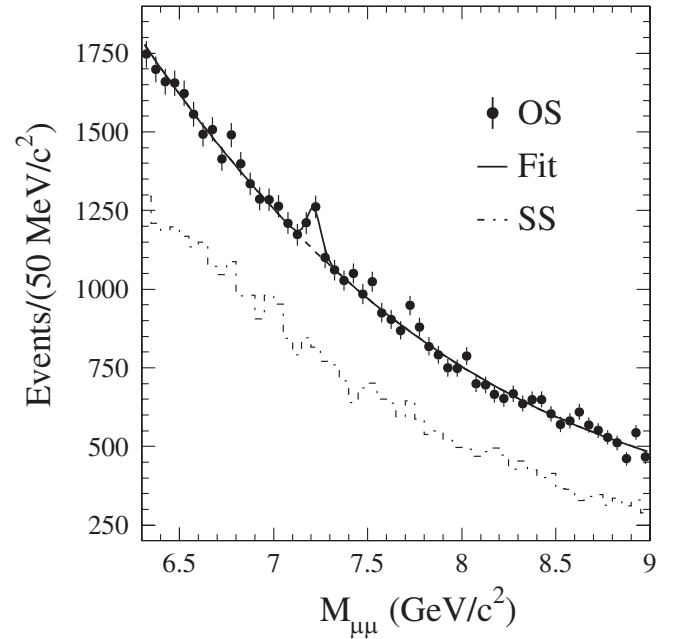


FIG. 4. Invariant mass distribution of opposite (\bullet) and same sign charge (dot-dashed) muon pairs which pass the isolation and impact parameter cuts. The solid line represents the fit described in Sec. VII.

ground, plus a Gaussian function, which searches for narrow resonances. We perform 54 fits, in which we constrain the Gaussian peak to the center of each of the 54 mass bins of Fig. 4; in each fit, we force the Gaussian width to the simulated resolution of the detector for that mass. For each mass bin, we use the integral of the Gaussian function and its error returned by the best fit to derive N_{ul} , the 90% credibility upper limit to the number of events contributed by a narrow resonance centered in that mass bin.³ We evaluate the ratio of the geometric and kinematic acceptance for an ε resonance to that for the $Y(1S)$ meson with the simulation described at the end of Sec. IV. In the event generator, an unpolarized resonance is produced with a flat rapidity distribution ($|y| \leq 1$) and a transverse momentum distribution that is rescaled from that of the $Y(1S)$ data so that $\langle p_T^\varepsilon \rangle / \langle p_T^{Y(1S)} \rangle = m_\varepsilon / m_{Y(1S)}$. For J/ψ mesons, this rescaling procedure predicts a $d\sigma/dp_T$ distribution that decreases more rapidly with increasing momenta than the distribution of the data. However, a poor modeling of the transverse momentum distribution is not a cause of error because the kinematic acceptance does not depend on the ε transverse momentum. As a cross-check, we also generated ε resonances using the shape of the transverse momentum distribution of the $Y(1S)$ data and verified that they return consistent acceptance values. The geometric

²The track impact parameter d is the distance of closest approach to the event primary vertex in the plane transverse to the beam line. The significance is defined as d/σ_d . The event primary vertex is determined as in the study in Ref. [16].

³The integral of the fit likelihood from N_{ul} to infinity is 10% of the integral of the fit likelihood from 0 to infinity. The justification for this procedure is Bayesian with a prior that is zero for negative resonance cross sections and flat for positive ones.

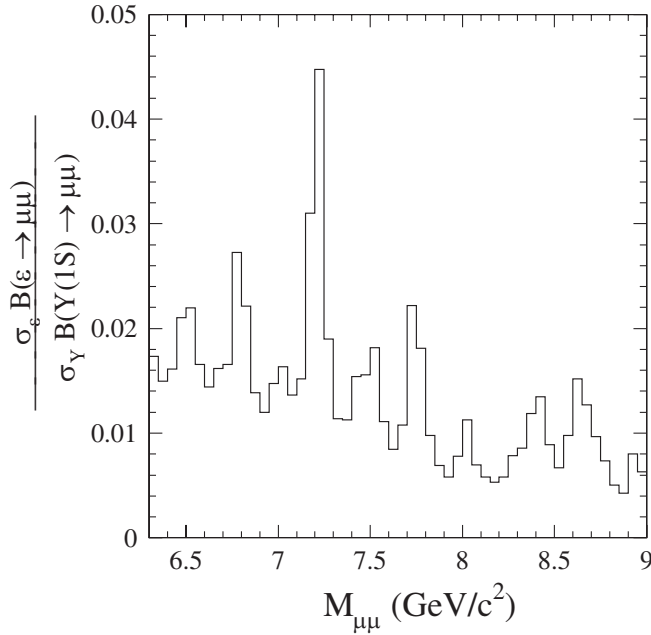


FIG. 5. Bayesian 90% upper limit to $\frac{\sigma_\epsilon B(\epsilon \rightarrow \mu\mu)}{\sigma_{Y(1S)} B(Y(1S) \rightarrow \mu\mu)}$ as a function of the ϵ mass.

and kinematic acceptance increases from 8.3% at 6.3 GeV/c² to 11.2% at 9.0 GeV/c² (it is 11.7% at Y(1S) mass). The parametrized correction factors for the trigger and reconstruction efficiencies, discussed at the end of Sec. IV, depend little on the muon p_T . Including these effects in the simulation, the acceptance is 4.7% at 6.3 GeV/c² and 6.3% at 9.0 GeV/c² (it is 6.6% at Y(1S) mass). The parametrized correction factors to the acceptance have approximately a 6% uncertainty. However, in the mass range considered in this study, the ratio of the simulated ϵ to Y(1S) acceptances is not affected by this uncertainty.

The ratio of N_{ul} to the number of observed Y(1S) mesons, corrected for the relative acceptance, provides the 90% credibility upper limit to $\sigma_\epsilon B(\epsilon \rightarrow \mu\mu) / \sigma_{Y(1S)} B(Y(1S) \rightarrow \mu\mu)$ shown in Fig. 5. Figure 6 shows the 90% credibility upper limit to Γ_i^ϵ derived using equation (1). We note that equation (1) tends to underestimate the ϵ production cross section. One can verify this by predicting the J/ψ production cross section from that of the Y(1S) meson that is about two order of magnitude smaller. The Y(1S) integrated cross section for $|y| \leq 0.6$ is measured to be 34.6 ± 2.5 nb⁴. The analogous cross section for the J/ψ meson is 3060 ± 460 nb⁵, whereas

⁴Average of the measurements in Refs. [14].

⁵We use the result reported in Ref. [17]. The measurement is performed at $\sqrt{s} = 1.96$ TeV, and we rescale the published value by the 10% expected increase of the cross section from 1.8 to 1.96 TeV [17]. We also extrapolate the result to $p_T^{\min} = 0$ GeV/c assuming that the fraction of prompt J/ψ mesons remains constant for transverse momenta smaller than 1.5 GeV/c.

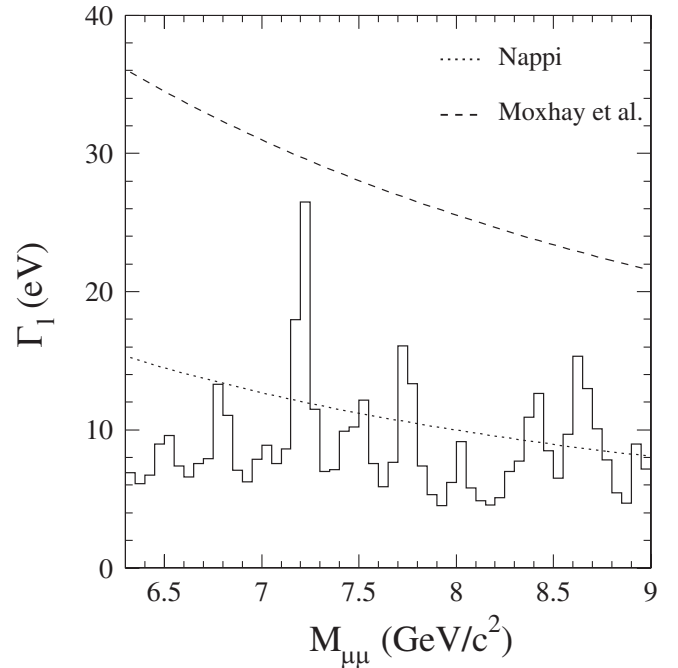


FIG. 6. Bayesian 90% upper limit to Γ_i^ϵ (histogram). The dashed and dotted lines represent the leptonic widths of 1^{--} bound states of scalar quark predicted in Refs. [5,9], respectively.

Eq. (1) predicts 1630 ± 116 nb. If the ϵ production cross sections predicted by Eq. (1) were also a factor of two smaller than the data, the Γ_i^ϵ limits set by our study would be a factor of two smaller than those indicated in Fig. 6.

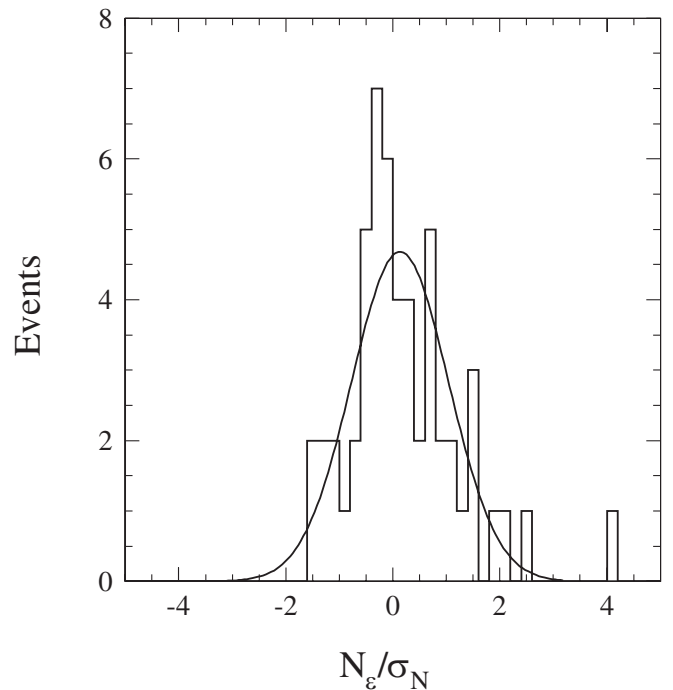


FIG. 7. Distribution of N_ϵ / σ_N (see text). The solid line is a Gaussian function with unit width.

Figure 7 shows the distribution of N_ε , the number of events attributed to a narrow resonance, divided by the error σ_N returned by the best fit for the 54 considered mass bins. With the exception of a point at 4.1σ , this distribution is consistent with a Gaussian function of unit width. Therefore, it seems fair to assume that the distribution of the 90% upper limits in Fig. 6 is statistically consistent with the average upper limit $\Gamma_i^\varepsilon = 8$ eV that corresponds to those cases with $N_\varepsilon/\sigma_N = 0$ in Fig. 7. The 4.1σ fluctuation occurs at the mass of 7.25 GeV/ c^2 .

VII. STUDY OF THE 7.25 GeV/ c^2 FLUCTUATION

In this section we explore the possibility that the anomalously large upper limit at 7.25 GeV/ c^2 is due to a real signal. A fit, which uses a Gaussian function with a fixed 38 MeV/ c^2 resolution, returns $M_\varepsilon = 7.22 \pm 0.01$ GeV/ c^2 and a signal of 250 ± 61 events over a smooth background of 3355 events, extrapolated in the 150 MeV/ c^2 region between 7.15 and 7.3 GeV/ c^2 (see Fig. 4). The probability that 3355 background events fluctuate to no less than 3605 is 8×10^{-6} (4.3σ). Since the mass range examined in Fig. 4 includes 52 almost independent combinations of three consecutive 50 MeV/ c^2 bins, the probability of obtaining an equal or larger statistical fluctuation in the inspected mass window is approximately 4.1×10^{-4} (3.5σ).

According to the simulation the acceptance for a 7.2 GeV/ c^2 resonance relative to that for the $Y(1S)$ meson is $A_\varepsilon = 0.78 \times A_{Y(1S)}$. It follows that

$$\sigma_\varepsilon B(\varepsilon \rightarrow \mu\mu) = (3.6 \pm 0.9) \times 10^{-2} \\ \times \sigma_{Y(1S)} B(Y(1S) \rightarrow \mu\mu).$$

We note that this value is in agreement with the theoretical expectation for a bound state of charge $-1/3$ squarks.

We have investigated three additional selection cuts that reduce the number of events by more than a factor of 2 and compare the effect of these cuts on the number of ε and $Y(1S)$ candidates:

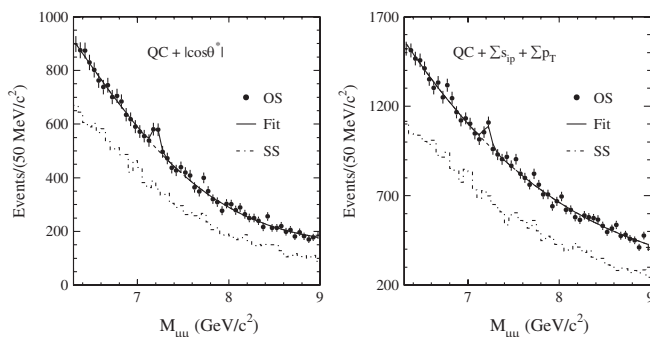


FIG. 8. Invariant mass distributions of muon pairs after applying the first and second cuts described in Table II. The solid line is a fit to the data described in the text.

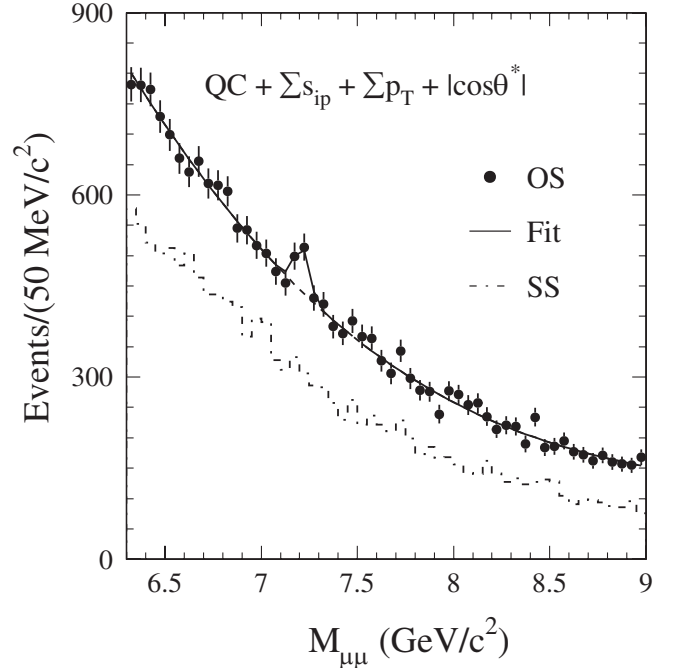


FIG. 9. Invariant mass distributions of opposite sign charge muon pairs after applying the third cut described in Table II.

TABLE II. Yield of ε and $Y(1S)$ candidates for different analysis cuts. The underlying backgrounds are fitted with polynomial functions and integrated over the mass ranges 7.15 – 7.3 and 9.3 – 9.55 GeV/ c^2 .

| Cut | ε | Background | $Y(1S)$ | Background |
|-----|------------------|------------|----------------|------------|
| QC | 249.7 ± 60.9 | 3355.0 | 9064 ± 118 | 1842 |
| # 1 | 160.5 ± 41.8 | 1508.0 | 3910 ± 90 | 611 |
| # 2 | 206.2 ± 57.0 | 2948.0 | 8667 ± 136 | 1587 |
| # 3 | 144.5 ± 39.0 | 1311.0 | 3699 ± 87 | 561 |

- (1) $|\cos(\theta^*)| \leq 0.4$, where θ^* is the polar angle between the μ^+ and ε directions in the ε center-of-mass system. This cut reduces the number of events by simply selecting a particular sector of the phase space.
- (2) $\sum_i p_{T_i} \leq 40$ GeV/ c and $\sum_j s_{ip}^j \leq 30$, where $\sum_i p_{T_i}^j$ is the scalar sum of the transverse momentum of all tracks i originating from the same vertex as the muon pair and $\sum_j s_{ip}^j$ is the sum of the impact parameter significance of all tracks j not used to define the primary vertex of the event [18]. This cut is intended to further suppress the heavy flavor background by rejecting events in which the muon pair carries a small fraction of the total transverse momentum or is produced in association with additional long-lived particles.
- (3) Cut 1 + cut #2.

The effect of these cuts is shown in Figs. 8 and 9, and is compared to the result for the $Y(1S)$ meson in Table II.

VIII. CONCLUSIONS

We have investigated the invariant mass spectrum of dimuons collected by the CDF experiment at the Tevatron collider to improve the limit to the existence of narrow resonances set by the experiments at the SPEAR e^+e^- collider. In the mass range $6.3 - 9.0 \text{ GeV}/c^2$, we derive 90% upper credible limits to the ratio of the production cross section times muonic branching fraction of possible narrow resonances to that of the $Y(1S)$ meson. In this mass range, the average limit varies from 1.7 to 0.5%. Assuming that $\sigma_e = \sigma_{Y(1S)} \times (m_{Y(1S)}/m_e)^3 \times \Gamma^e/\Gamma^{Y(1S)}$, these limits correspond to an average 90% upper credible limit of 8 eV to the leptonic width of possible resonances. An exception is the mass region around $7.2 \text{ GeV}/c^2$ where

we observe a bump of 250 ± 61 events with a width consistent with the detector resolution. The size of the excess is consistent with the theoretical expectation for the production of a $1^{--} p$ -wave resonance but its statistical significance (3.5σ) is not sufficient to claim the discovery of a new particle.

ACKNOWLEDGMENTS

We thank the Fermilab staff, the CDF Collaboration, and their technical staff for their contributions. This work was supported by the US Department of Energy and National Science Foundation; the Istituto Nazionale di Fisica Nucleare; and the Ministry of Education, Culture, Sports, Science, and Technology of Japan.

-
- [1] M. Carena *et al.*, Phys. Rev. Lett. **86**, 4463 (2001).
 - [2] S. Eidelman *et al.*, Phys. Lett. B **592**, 1 (2004).
 - [3] P. Janot, Phys. Lett. B **594**, 23 (2004).
 - [4] D. G. Aschman *et al.*, Phys. Rev. Lett. **39**, 124 (1977); A. M. Boyarsky *et al.*, Phys. Rev. Lett. **34**, 762 (1975); R. F. Schwitters in *Proceedings of the XVIII International Conference on High Energy Physics, Tbilisi, 1976*, edited by N. N. Bogoliubov *et al.*, (JINR, Dubna, U.S.S.R., 1977).
 - [5] C. Nappi, Phys. Rev. D **25**, 84 (1982).
 - [6] T. Appelquist and H. D. Politzer, Phys. Rev. Lett. **34**, 43 (1975); E. Eichten *et al.*, Phys. Rev. D **17**, 3090 (1978).
 - [7] F. Abe *et al.*, Nucl. Instrum. Methods Phys. Res., Sect. A **271**, 387 (1988).
 - [8] V. Barger and R. Phillips, *Collider Physics* (Addison-Wesley, Reading, MA, 1987).
 - [9] P. Moxhay *et al.*, Phys. Lett. B **158**, 170 (1985).
 - [10] F. Abe *et al.*, Phys. Rev. Lett. **83**, 3378 (1999); Phys. Rev. D **60**, 051101 (1999); Phys. Rev. D **57**, R3811 (1998); Phys. Rev. D **55**, 2546 (1997).
 - [11] F. Abe *et al.*, Phys. Rev. D **57**, 5382 (1998); Phys. Rev. D **55**, 1142 (1997).
 - [12] F. Abe *et al.*, Phys. Rev. Lett. **73**, 225 (1994).
 - [13] D. Kestenbaum, Ph.D. thesis, Harvard University, 1996 (unpublished).
 - [14] D. Acosta *et al.*, Phys. Rev. Lett. **88**, 161802 (2002); F. Abe *et al.*, Phys. Rev. Lett. **75**, 4358 (1995).
 - [15] T. Affolder *et al.*, Phys. Rev. D **64**, 032002E (2001); **67**, 119901 (2003).
 - [16] D. Acosta *et al.*, Phys. Rev. D **69**, 012002 (2004).
 - [17] D. Acosta *et al.*, Phys. Rev. D **71**, 032001 (2005).
 - [18] Tracks with impact parameter significance smaller than 3 are used to reconstruct the primary vertex; we reject tracks with impact parameter larger than 0.15 cm.